Sensors and Materials, Vol. 36, No. 9 (2024) 3691–3700
MYU Tokyo

S & M 3759

Examination of Slit Defect Inspection Method for Steel Bars Using Only DC Magnetic Field with the Velocity Effect

Masafumi Kuromizu[1*] and Yuji Gotoh[2]

[1]Graduate School of Engineering, Oita University,
700 Dannoharu, Oita 870-1192, Japan
[2]Faculty of Science and Technology, Oita University,
700 Dannoharu, Oita 870-1192, Japan

(Received May 30, 2024; accepted July 17, 2024)

Keywords: non-destructive inspection, velocity effect, ferromagnetic materials, static magnetic field, eddy current, 3D nonlinear FEM, electromagnetic sensors

C45, a ferromagnetic material, can be strengthened by heat treatment such as quenching and is widely used as a material for general mechanical parts such as springs in automobiles. However, the presence of defects or flaws can cause cracking during the quenching stage, and a high-speed inspection method for detecting defects is required. In this study, we proposed and examined an inspection method for detecting defects using only a DC magnetic field by moving a round steel bar material at a high speed of 1 m/s inside a ring-shaped permanent magnet and generating eddy currents due to the velocity effect.

1. Introduction

Round-bar C45 steel is induction-hardened to increase its strength and is often used as a material for automotive springs and general machine parts. However, if defects or flaws exist at the induction hardening stage, cracking may occur during the quenching stage. Even if cracking does not occur during the quenching stage, there are concerns about various problems such as the shortening of the life of the product or causing it to fail. Eddy current testing[(1–3)] using a penetrating coil and flux leakage testing[(4)] are examples of defect inspection methods for round steel bars. However, the sensitivity of these testing methods decreases when the test specimen is moving at a high speed. Generally, steel bar material moves at a speed of 0.6 to 1.0 m/s on an inspection line. Therefore, it is difficult to select the optimum testing conditions for these testing methods. On the other hand, it is known that when a ferromagnetic round steel bar is moved at a high speed with an applied static magnetic field, eddy currents are generated in the ferromagnetic round steel bar, which is similar to eddy current testing.[(5–7)] This method can be performed with inexpensive testing equipment because the test sensor should be composed of only a permanent magnet and a detection coil. However, the detailed inspection principle of this method has not yet been clarified. In this research, we prepared a test specimen of a C45 steel bar, which is commonly used for automobile springs. This specimen had artificial defects introduced into it

*Corresponding author: e-mail: v23f1001@oita-u.ac.jp
https://doi.org/10.18494/SAM5162

ISSN 0914-4935

before hardening. Then, the inspection methods designed to detect these defects were evaluated. The inspection method utilizes the velocity effect,[8] which arises when the specimen is moved at a speed of 1 m/s inside a ring-shaped permanent magnet. A detection coil wrapped around the inner surface of the magnet detects changes in magnetic flux due to defects.

The inspection principle is clarified by nonlinear electromagnetic field analysis using a three-dimensional finite element method (3D-FEM), and the usefulness of this inspection method is demonstrated through verification experiments.

2. Sensor Model and Analysis Method

2.1 Sensor model configuration

Figure 1 shows the inspection model in a bird's eye view and a 1/2 region area. The proposed sensor consists of a ring-shaped permanent magnet (neodymium magnet) with a surface magnetizing force of 0.48T and the detection coil wrapped around the inner surface of the magnet. The dimensions of the permanent magnet are an inner diameter φ_r of 18 mm, an outer diameter φ_R of 32 mm, and a height h of 8 mm in the z-direction. The detection coil with 120 turns is placed inside the permanent magnet with φ_r of 17.2 mm, φ_R of 18.0 mm, and h of 3.0 mm in the z-direction. The diameter of the inspected steel bar of C45 material is 9 mm, and the length in the z-direction is 1000 mm. The outer surface of the steel bar material has a slit defect. The defect width is constant at 2.0 mm in the z-direction, and the defect depth varies as 0.5, 2.0, and 5.0 mm in the x-direction. The inspected steel bar material is inserted inside the permanent magnet and moved at a speed of 1 m/s in the +z-direction. In the analysis, the permanent magnet is moved at a speed of 1 m/s in the −z-direction to simulate the relative movement of the inspected steel bar material in the +z-direction.

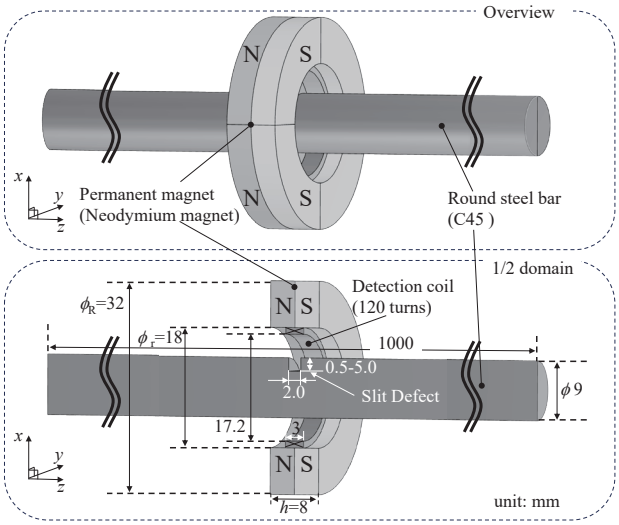

Fig. 1. Sensor model (1/2 region).

2.2 Electromagnetic field analysis considering velocity term

In this study, the distributions of the magnetic flux and eddy current densities are obtained by the nonlinear analysis of the inspected steel bar material (C45). This numerical calculation is performed using a 3D-FEM taking into account the initial magnetization curve and electrical conductivity. The basic equations in the electromagnetic field analysis, considering eddy currents by the A-φ method, are as follows.

$$\mathrm{rot}\left(\nu\,\mathrm{rot}\boldsymbol{A}\right)=\boldsymbol{J}_0-\sigma\left(\frac{\partial\boldsymbol{A}}{\partial t}+\mathrm{grad}\;\phi\right) \tag{1}$$

$$\mathrm{div}\,\boldsymbol{J}_\mathrm{e}=\mathrm{div}\left\{-\sigma\left(\frac{\partial\boldsymbol{A}}{\partial t}+\mathrm{grad}\;\phi\right)\right\}=0 \tag{2}$$

Here, A is the magnetic vector potential, φ is the electric scalar potential, σ is the electrical conductivity, ν is the magnetic resistivity, and J_0 is the current density.

The electromagnetic field analysis that takes velocity effects into account will be explained below using the model shown in Fig. 2, without taking into account the gradφ terms of Eqs. (1) and (2) for simplicity. In a transient analysis in which a permanent magnet generating a DC magnetic field is moved along an inspected steel bar over time, the time derivative $\partial A/\partial t$ in the moving coordinate system can be discretized using the backward difference method as follows.[9,10]

$$\frac{\partial A\left(z_2\right)^{t+\Delta t}}{\partial t}\cong\frac{A^*\left(z_2\right)^{t+\Delta t}-A\left(z_1\right)^t}{\Delta t} \tag{3}$$

Here, Δt indicates the time interval, z_1 is an optional position of the permanent magnet, and z_2 is the position of the permanent magnet after Δt from the position of z_1. $A(z_2)^{t+\Delta t}$ on the left side

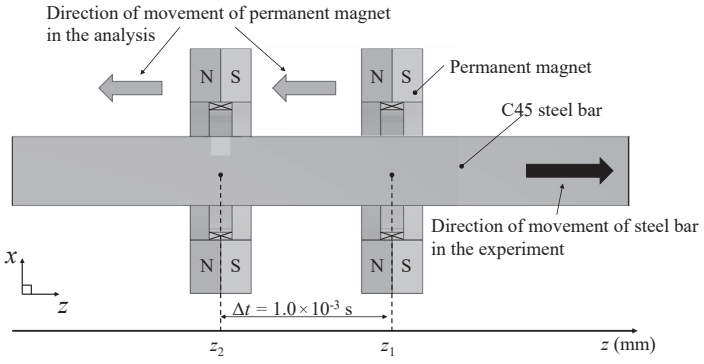

Fig. 2. Direction of movement of electromagnetic sensor.

represents the magnetic vector potential at Δt seconds after any time t. Superscript (*) denotes unknown variables. The speed of the inspected steel bar material moving inside the permanent magnet is 1 m/s. The pitch of movement in the analysis is 1 mm/step. Therefore, the time interval Δt in the step-by-step method is 1.0×10^{-3} s. The initial magnetization curve of the inspected steel bar material (C45) is shown in Fig. 3. In this analysis, the Newton–Raphson method (N–R method) is used for nonlinear iterative calculation considering the magnetic properties shown in Fig. 3. The incomplete Cholesky conjugate gradient method (ICCG method) is used to converge the calculation results. The conditions of the analysis performed in this study are shown in Table 1.

3. Analysis Results

3.1 Density distribution of eddy currents due to velocity effects

Figure 4 shows the eddy current density distribution generated in the steel bar material for only one layer in the *y*-direction when the defect-free steel bar material moves at 1 m/s in the +*z*-direction. If the steel bar material is not moving, the DC magnetic flux density inside the steel bar from the permanent magnet is distributed in the +*z*-direction. When the steel bar moves

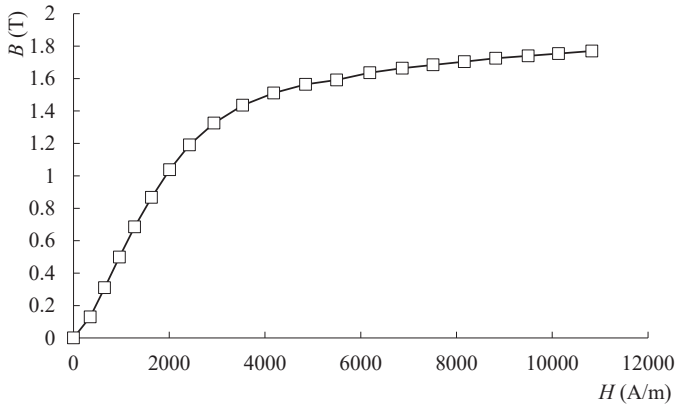

Fig. 3. Initial magnetization curve (C45).

Table 1
Conditions of the analysis

Conductibliity (C45)	4.95×10^6 S/m
Surface magnetization	0.48 T
Detection coil	0.1ϕ, 120 turns
Lift-off distance	4.1 mm
Movement speed	1 m/s
Number of nodes	170542
Number of elements	162543
Convergence criterion	N-R method: 1.0×10^{-4} T ICCG method: 1.0×10^{-6}

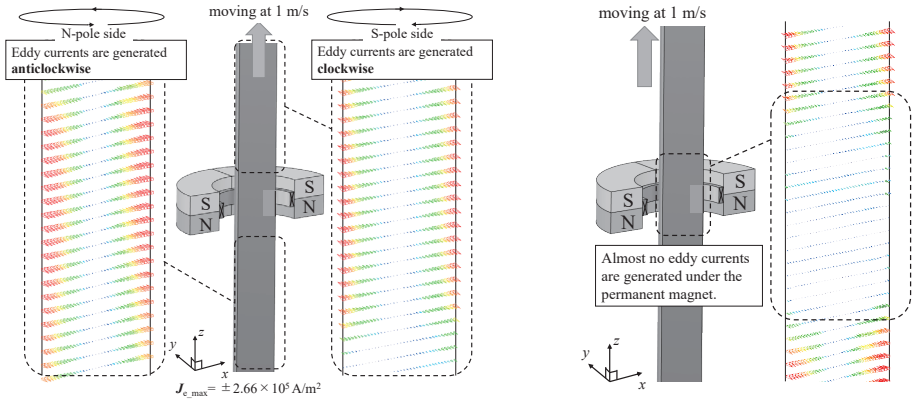

(a) (b)

Fig. 4. (Color online) Eddy current density distribution in the C45 steel bar material: (a) near the N- and S-poles of the permanent magnet and (b) directly under the permanent magnet.

at a high speed in the +z-direction, eddy currents are generated inside the steel near the S-pole of the permanent magnet, inducing an N-pole. This weakens the DC magnetic flux density from the permanent magnet. On the other hand, when eddy currents are generated inside the steel bar near the N-pole of the permanent magnet, an S-pole is induced. This also weakens the DC magnetic flux density from the permanent magnet. The direction of eddy current generation is reversed inside the steel bar near the N- and S-pole sides of the permanent magnet. Figure 4(b) shows the distribution of eddy current density inside the steel bar directly under the permanent magnet. There are almost no eddy currents directly inside the steel bar under the permanent magnet. This is because the DC magnetic field due to the permanent magnet is dominant.

3.2 Magnetic flux density distribution during constant velocity movement

Figure 5 shows the calculated magnetic flux density distribution inside the steel bar material when the steel bar is moving at a speed of 1 m/s in the +z-direction. Figure 5(a) shows the magnetic flux density distribution inside the steel bar near the N- and S-pole sides of the permanent magnet. This figure indicates that the magnetic flux density decreases at the center of the steel bar near the N-pole side of the permanent magnet. This is because eddy currents generate a magnetic field that cancels the magnetic flux density from the N-pole of the permanent magnet, as shown in the eddy current distribution on the left side of Fig. 4(a). On the other hand, the magnetic flux density increases at the center of the steel bar near the S-pole side. This is because eddy currents generate a magnetic field that increases the magnetic flux density from the S-pole of the permanent magnet, as shown in the eddy current distribution on the right side of Fig. 4(a). Figure 5(b) shows the magnetic flux density distribution generated inside the steel bar material directly under the permanent magnet. The magnetic flux is uniformly distributed directly under the permanent magnet because the DC flux due to the permanent magnet is dominant and eddy current generation is low.

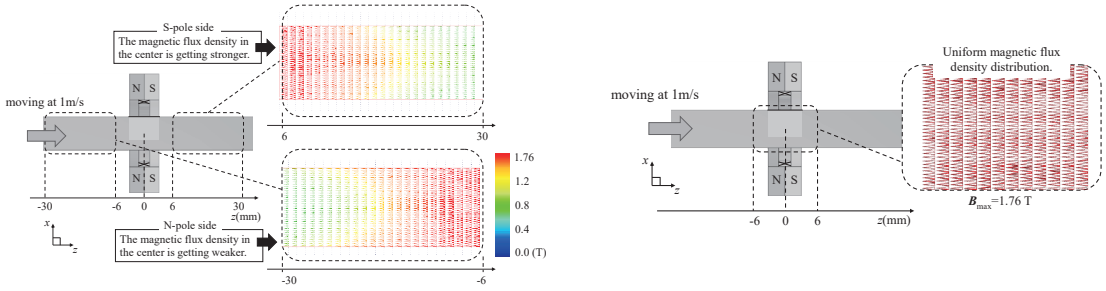

(a) (b)

Fig. 5. (Color online) Magnetic flux density distribution in the C45 steel bar material: (a) near the N- and S-poles of the permanent magnet and (b) directly under the permanent magnet

4. Verification of Defect Inspection by Analysis and Experiment

In this section, a comparative verification between analysis and experiment is performed on the model to detect defects shown in Fig. 6. Slit-like defects with a width of 2.0 mm in the z-direction and depths of 0.5, 2.0, and 5.0 mm were formed in steel bar specimens. The center of a slit defect is set at $z = 0$ mm and moved from $z = 50$ to -50 mm. In the analysis, the permanent magnet and detection coil are moved at a pitch of 1 mm in the $-z$-direction at 1 m/s, and the average magnetic flux density in the detection coil is calculated at each moving point. The verification experiments are conducted using the experimental setup shown in Fig. 7. It consists of the C45 steel bar, the permanent magnet, and the detection coil in concentric circles, and the C45 steel bar is moved at a speed of 1m/s by the electric cylinder. The inside of the jig fixing the permanent magnet and detection coil is shown in Fig. 7(b). The detection coil is wound with 120 turns as in the analysis.

In the experiment, the induced electromotive force generated by the movement of the steel bar material is acquired by the detection coil, converted to magnetic flux density by integrating the voltage waveform over time, and compared with the analysis value.

Figure 8 shows the amount (DB_z) of change in magnetic flux density obtained within the detection coil for each defect depth. The horizontal axis of the figure shows the moving distance of the steel bar, and the vertical axis shows the amount (DB_z) of change in magnetic flux density from the magnetic flux density in the detection coil at a location where no defect exists. Figure 8(a) shows the calculated results, and Fig. 8(b) shows the actual measurement results. These figures denote that the magnetic flux density B_z in the detection coil decreases at z = 0 mm where defects exist. When the defect depth increases, the amount of decrease in magnetic flux density also increases. In addition, the calculated results in Fig. 8(a) and the measured results in Fig. 8(b) show similar trends.

The reason why the magnetic flux density B_z in the detection coil decreases when a defect exists in this inspection method is investigated. Figure 9 shows the distribution of the magnetic flux density inside the steel bar material with and without defects under the permanent magnet.

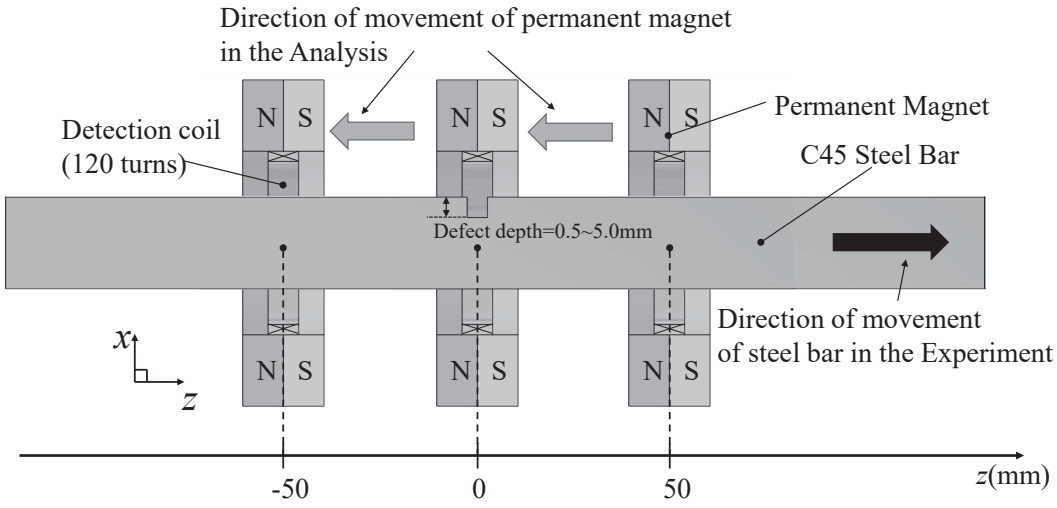

Fig. 6. Comparative model of experiment and analysis.

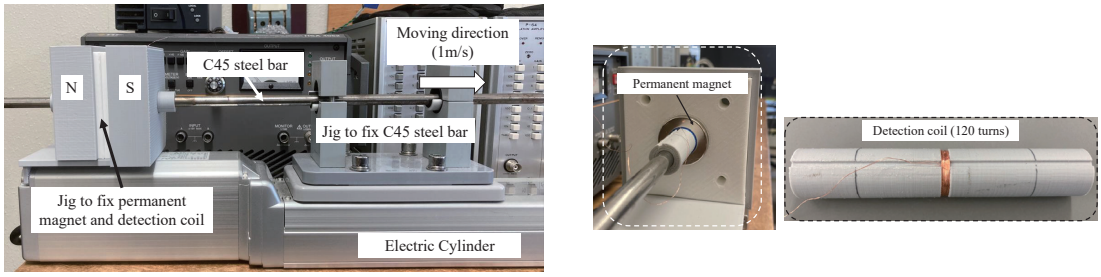

(a) (b)

Fig. 7. (Color online) Appearance of experimental equipment: (a) overall view of the experimental setup and (b) permanent magnet and detection coil part.

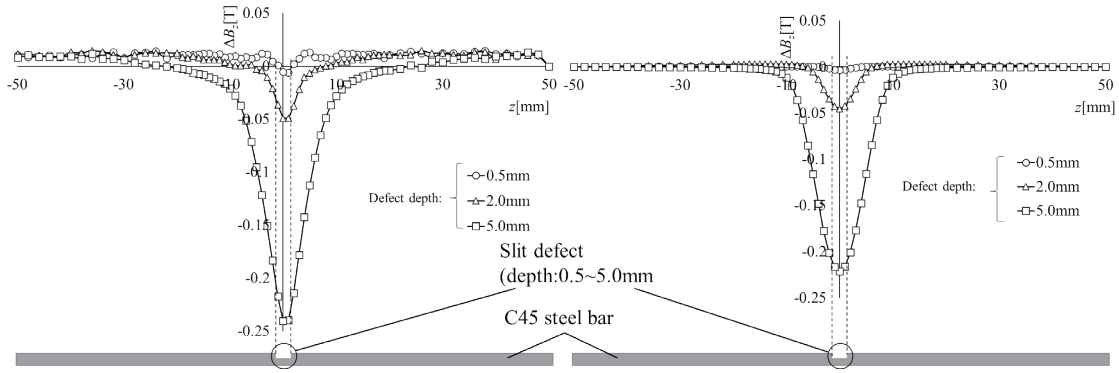

(a) (b)

Fig. 8. Changes in magnetic flux density Bz inside the detection coil in analysis and experiment: (a) analysis and (b) experiment results.

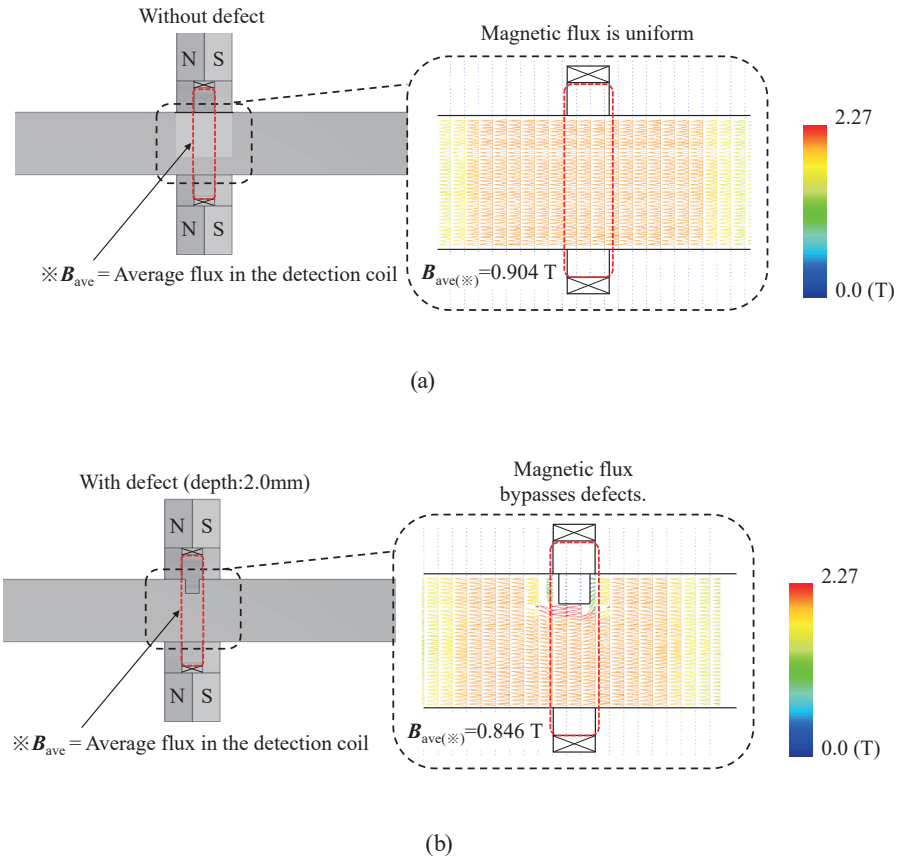

Fig. 9. (Color online) Effects of defect on magnetic flux (a) without and (b) with defects.

As shown in Fig. 9(a), if there is no defect in the steel bar, the magnetic flux density inside the steel bar is uniformly distributed in the *z*-direction. However, if there is a defect on the surface of the steel bar, the magnetic flux is distributed to bypass the defects, as shown in Fig. 9(b). Therefore, the magnetic flux density within the steel bar is no longer uniformly distributed in the *z*-direction.

Since the detection coil detects the magnetic flux in the *z*-direction, the obtained magnetic field along the *z*-direction in the detection coil decreases when there is a defect in the steel bar.

5. Defect Signal Variation with Speed Change

In defect inspection using the velocity effect, it is clear that changes in movement speed significantly affect the defect signal. Figure 10 shows the variation of the defect signal at the speed of movement. The figure shows that the amplitude of the defect signal increases with the speed of movement. This is because the higher speed of movement increases the change in magnetic flux per unit of time. In addition, the defect signal spreads in the time axis direction as the speed of movement decreases.

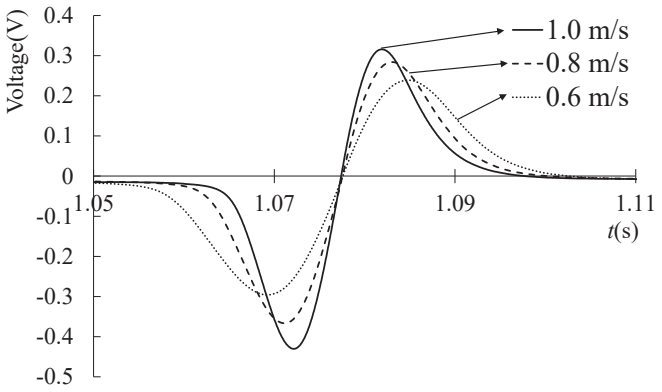

Fig. 10. Defect signal waveform at speed of movements.

6. Conclusions

The results obtained are summarized as follows.

(1) In the proposed inspection method, only a DC magnetic field is used, with the velocity effect generating eddy currents in the inspected steel bar material as it passes through the permanent magnet. The direction of the eddy currents is reversed near each pole of the permanent magnet.

(2) The magnetic flux density generated inside the steel bar directly under the permanent magnet is uniformly distributed in the axial direction of the steel bar. Therefore, the magnetic flux density of the axial component of the steel bar decreases. The detection signal of the detection coil that detects the magnetic field in the axial direction of the steel bar also decreases.

(3) A comparison of the electromagnetic field analysis using the three-dimensional finite element method and the verification experiment shows a similar trend, indicating the usefulness of the proposed method.

References

1 D. G. Park, C. S. Angani, G. D. Kim, C. G. Kim, and Y. M. Cheong: IEEE Trans. Magn. **45** (2009) 3893.
2 M. Rebican, Zhenmao Chen, N. Yusa, L. Janousek, and K. Miya: IEEE Trans. Magn. **42** (2006) 1079.
3 C. S. Angani, H. G. Ramos, A. L. Ribeiro, T. J. Rocha, and P. Baskaran: IEEE Trans. Magn. **52** (2016) 1.
4 Y. Gotoh and N. Takahashi: IEEE Trans. Magn. **42** (2006) 1415.
5 R. Schmidt, J. M. Otterbach, M. Ziolkowski, H. Brauer, and H. Toepfer: IEEE Trans. Magn. **54** (2018) 1.
6 H.-J. Shin, J.-Y. Choi, H.-W. Cho, and S.-M. Jang: IEEE Trans. Magn. **49** (2013) 4152.
7 J. Wu, Y. Sun, B. Feng, and Y. Kang: IEEE Trans. Magn. **53** (2017) 1.
8 M. Tohara, M. Kuromizu, and Y. Gotoh: Sens. Mater. **33** (2021) 2867.
9 K.Muramatsu, T.Nakata, N.Takahashi, and K.Fujiwara: IEEE Trans. Magn. **28** (1992) 1186.
10 K.Muramatsu, T.Nakata, N.Takahashi, and K.Fujiwara: IEEE Trans. Magn. **32** (1996) 749.

About the Authors

Masafumi Kuromizu graduated from Kyushu Polytechnic College, Japan, in 2021. He received his M.E. degree from Oita University, Japan, in March 2023. Since April 2024, he has been working as an assistant at the Polytechnic University and is engaged in research as part of the doctoral program at Oita University. His main research interest is in the development of electromagnetic non-destructive inspection methods for steel materials.
(v23f1001@oita-u.ac.jp)

Yuji Gotoh received his B.E. and M.E. degrees from Polytechnic University, Japan, in 1996 and 1998, respectively, and his Ph.D. degree from Okayama University, Japan, in 2002. He is presently a professor in the Faculty of Science and Technology, Oita University. His main research interest is in the development of electromagnetic non-destructive inspection methods for steel materials.